한국기계가공학회지, 제17권, 제6호, pp.75～82(2018.12) ISSN 1598-6721(Print)
Journal of the Korean Society of Manufacturing Process Engineers, Vol. 17, No. 6, pp.75~82(2018.12) ISSN 2288-0771(Online)

https://doi.org/10.14775/ksmpe.2018.17.6.075

Structural Optimization of an LMU Using Approximate Model

Dong-Seop Han*, Si-Hwan Jang**, Soon-Hyeong Park***, Kwon-Hee Lee**,#
*R&D Center, Remitite Co., **Department of Mechanical Engineering, Dong-A University,
***Technical Center, Central Corporation

근사모델을 이용한 LMU의 구조최적설계

한동섭*, 장시환**, 박순형***, 이권희**,#
*(주)레미타이트 기업부설연구소, **동아대학교 기계공학과, ***㈜센트랄 중앙연구소

(Received 23 August 2018; received in revised form 27 August 2018; accepted 30 August 2018)

ABSTRACT

This study suggests an optimal design process of an LMU, which is installed on the top side of offshore structures. The LMU is consist of EB(elastomeric bearing) and steel plate, and supports the vertical loads of offshore structures and assists its stable installation. The structural design requirement of the LMU is related to its stiffness. This study utilizes the finite element analysis to predict the stiffness. The stiffness of the EB depends on the size of the bearing. Thus, the design variables in this study are defined as the thickness, the width and the number of plates. Since the LMU has different loads for different locations, its stiffness should be designed differently. The multiobjective function is introduced to attain the target stiffness. In this process, the metamodel using the kriging interpolation method is adopted to replace the true stiffness.

Key Words : Leg Mating Unit(LMU, 레그 조합 유닛), Stiffness(강성), Top Side(탑사이드), Finite Element Analysis(유한 요소 해석), Elastomeric Bearing(EB, 탄성체 베어링), Kriging (크리깅)

1. Introduction

A leg mating unit (LMU) is a structure used to absorb loads and install a structure stably, as it is placed at the supporting point of the topside in a marine structure[1]. Generally, an LMU is a cylindrical shape, in which an elastomeric bearing and reinforced steel plate are alternately laminated, and a rubber pad is mounted on the lower lateral side[1]. Since loads applied differ at every supporting point in marine structures, the LMU should have the same displacement in all installation locations. That is, the compressive stiffness at each point should be designed differently[1].

The stiffness of an LMU is dependent on the size of the bearing as well as the number and size of the reinforced plates laminated on the inside. A previous study[1] predicted the stiffness of an LMU through finite element analysis (FEA) and investigated the relationship between reinforced plates and compressive stiffness. To do this, the stiffness was evaluated through FEA while changing the thickness, width, and number of reinforced steel plates. However, the study was limited to designing

Corresponding Author : leekh@dau.ac.kr
Tel: +82-51-200-7638, Fax: +82-51-200-7656

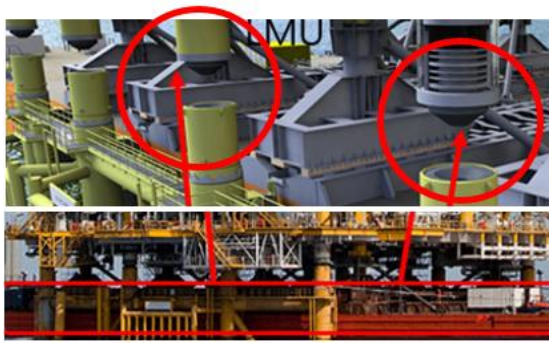

Fig. 1 Leg mating unit

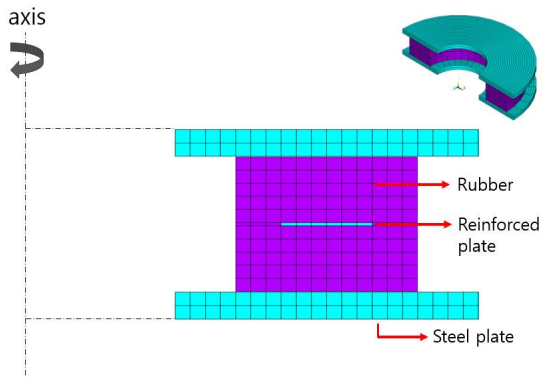

Fig. 2 Example of finite element model

an LMU with trial and error method. Thus, the present study aims to propose and apply an optimal design technique for an LMU by extending the previous study.

The thickness, width, and number of reinforced plates were set as the design variables for the optimal design of the elastomeric bearing in the LMU. The elastomeric bearing[2] plays a role as a shock absorber, and its stiffness design is important. Here, the number of reinforced steel plates is a discrete design variable. Every location where the LMU is placed has its own goal stiffness. Thus, a multi-objective function was employed to consider this. The stiffness at each location was predicted using a metamodel in this process. A Kriging interpolation method[3-6] was used to create the metamodel, which was implemented by Excel. The optimal solution in the multi-objective function was calculated by using the built-in generalized reduced gradient algorithm in Excel. This study used the commercial program ANSYS for FEA.

2. Structure of LMU and evaluation of stiffness

This study proposed a design of an LMU with optimal stiffness used to install a topside of a marine structure, as shown in Fig. 1. Most LMUs are cylindrical shaped, and the reinforced plate-inserted rubber elastomeric bearing and steel plate are laminated in layers.

The LMU in this study had an axisymmetric shape, which is equivalent to a two-dimensional (2D) axisymmetric simple model for FEA, as shown in Fig. 2. The material of the elastomeric bearing in the LMU was viscoelastic, and a force-displacement curve had to be made to calculate the compressive stiffness. This was done by calculating the reaction force (RF) by inputting a displacement as a load. The coefficient of friction in the boundary between the lower and upper steel plates was set to 0.1, and the contact capability of ANSYS was applied[1].

3. Application of metamodel-based optimization

3.1 Metamodel-based optimization

The metamodel is generally used to calculate optimal solutions if shape variables are complex, the sensitivity analysis is difficult, a discrete design is included, or the FEA time is too long in the structural optimal design. The stiffness analysis of the LMU should consider the contact phenomenon, and discrete design variables are included in the design. Thus, this study adopted the metamodel-based

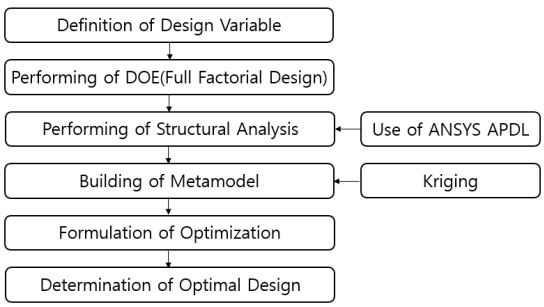

Fig. 3 Optimization process based on metamodel method

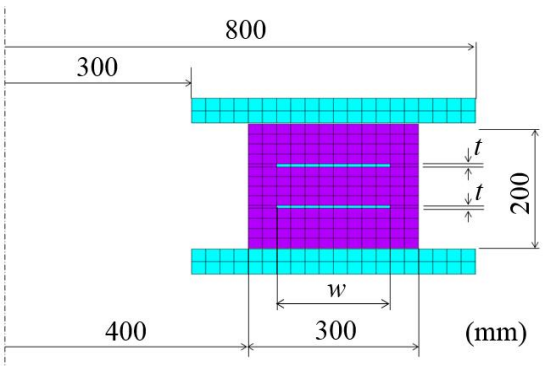

Fig. 4 Section of EB and definition of design variable

optimization technique for the LMU design. The metamodel can be built using a Kriging model[3-6] and a response surface model[7], etc.

This optimization process is shown in Fig. 3. First, design variables were defined, and experiments were set to build a metamodel using the experimental design. Here, a full factorial experiment was used. In addition, FEA was performed for each experiment. ANSYS was used to calculate the stiffness in this study. Next, based on the analysis results, a Kriging interpolation method was employed to build an approximate model. The multi-objective function was substituted with the approximate model, and finally, the optimal solution was calculated using the generalized reduced gradient (GRG) algorithm in the solution search function, a built-in function in Excel. In addition, verification analysis was performed to calculate the actual value in the optimal solution, since the predicted optimal solution was based on the approximate model.

3.2 Formulation for optimal design

The cross-section of the elastomeric bearing model in this study is shown in Fig. 4. The design variables considered in the optimization are related to the steel plate inside of the elastomeric bearing. As shown in the figure, the thickness (t), width (w) and number of steel plates (n) are defined as the design variables. For example, a model with two reinforced plates is shown. The design variables are selected based on the results in [1].

The formulation for the optimal design can be described as follows:

$$\textbf{Minimize}\quad R=\sum_{i=1}^{p} w_f(\hat{y_i}-y_t)^2 \quad (i=1,2,...,p) \qquad (1)$$

$$\textbf{Subject to}\quad \begin{aligned} 3 \le t\,(mm) \le 9 \\ 100 \le w\,(mm) \le 200 \\ 1 \le n(ea) \le 3 \end{aligned}$$

Here, p is 6, which is the maximum displacement load 60 mm divided by 10 mm. y_t refers to the goal RF (stiffness) at the divided displacement load, and $\hat{y_i}$ refers to the RF (stiffness) predicted with the Kriging approximation model at the given displacement load. Design variables t and w are continuous design variables and design variable n is a discrete design variable. In Section 3, the Kriging approximation model is first calculated with regard to $\hat{y_i}$ for each displacement load. That is, a RF in response to each displacement is indicated as a design variable.

3.3 Design of experiments

This study employed a full factorial experiment

Table 1 Levels of design variables

Levels\ DV	*t*(mm)	*w*(mm)	*n*(ea)
1	3	100	1
2	6	150	2
3	9	200	3

method for each design variable as a design of experiment method. The level of each design variable was set to 3, as presented in Table 1, so that $3^3 = 27$ experiments were defined.

3.4 Kriging model

In the Kriging model, a global approximation model is predicted as follows[3-6].

$$\hat{f}(\mathbf{x}) = \hat{\beta} + \mathbf{r}^T(\mathbf{x})\mathbf{R}^{-1}(\mathbf{f} - \hat{\beta}\,\mathbf{q}) \tag{2}$$

Here, **x** refers to the design variable vector (**x**=[*t*, *w*, *n*] in this study), ^ refers to an estimate, $\hat{f}$ is the predicted response($\hat{y}_i$ in this study), $\mathbf{R}^{-1}$ refers to the inverse matrix of correlation matrix **R**, **r** refers to the correlation matrix, **f** refers to the response value vector, **q** refers to the unit vector, and ß refers to the constant. The correlation vector can be defined as follows:

$$R(\mathbf{x}^j, \mathbf{x}^k) = Exp\left[-\sum_{i=1}^{n_v}\theta_i\left|x_i^j - x_i^k\right|^2\right], \quad (j = 1,\ldots,n_s, k = 1,\ldots,n_s) \tag{3}$$

Here, Θ refers to a parameter that can be calculated by following the optimization, and it equals the number of design variables.

$$maximize \quad -\frac{[n_s ln(\hat{\sigma}^2) + ln|\mathbf{R}|]}{2}, \tag{4}$$

A more detailed description of Kriging theory and induction can be found in [3-6].

3.5 Generation of Kriging model

Table 2 Parameters of θ and β

d(mm)	Parameter	$\hat{y}_i$ (RF: kN, *i*=1,..,6)
10	θ_1	0.01
	θ_2	0.055
	θ_3	0.153
	β	1748.16
20	θ_1	0.0598
	θ_2	0.416
	θ_3	0.564
	β	3015.69
30	θ_1	0.037
	θ_2	0.875
	θ_3	0.745
	β	5012.42
40	θ_1	0.012
	θ_2	0.512
	θ_3	0.45
	β	9488.99
50	θ_1	0.023
	θ_2	0.119
	θ_3	0.67
	β	14964.83
60	θ_1	0.02
	θ_2	0.185
	θ_3	0.656
	β	28805.97

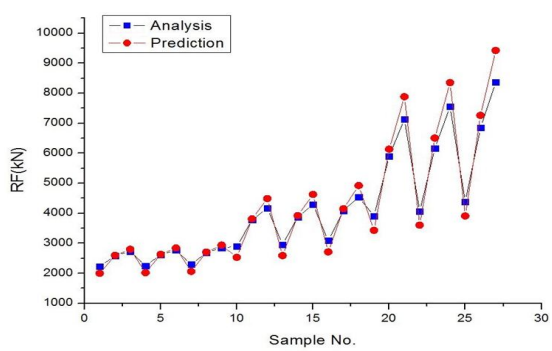

Fig. 5 Comparison of prediction and analysis at d=30mm

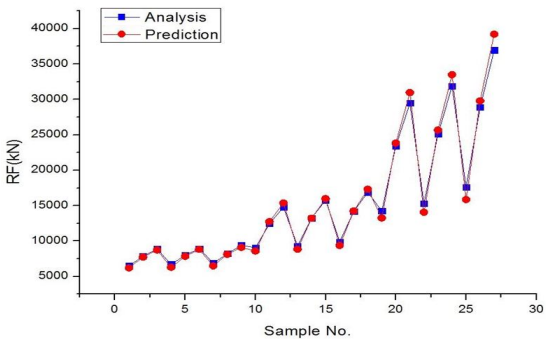

Fig. 6 Comparison of prediction and analysis at d=60mm

Table 3 Test points for model validation

No.	*t*(mm)	*w*(mm)	*n*(ea)
1	4	120	1
2	4	160	1
3	4	180	1
4	5	120	1
5	5	160	1
6	5	180	1
7	7	120	1
8	7	160	1
9	7	180	1
10	4	120	2
11	4	160	2
12	4	180	2
13	5	120	2
14	5	160	2
15	5	180	2
16	7	120	2
17	7	160	2
18	7	180	2
19	4	120	3
20	4	160	3
21	4	180	3
22	5	120	3
23	5	160	3
24	5	180	3
25	7	120	3
26	7	160	3
27	7	180	3

Table 2 presents the parameter values in the Kriging approximate model created every 10 mm from 10 mm to 60 mm of displacement load. The Kriging predicted value in the RF can be calculated by substituting each parameter value in Table 2 into Eq. (2).

To validate of the Kriging model, 27 arbitrary de sign points were created within the design variable r ange as presented in Table 3, and predicted and tru e analysis values were compared at those points. Th e displacement load values considered important in t his study were 30 mm and 60 mm. The errors betw een the structural analysis results and predicted valu es in the Kriging approximate model are shown in Figs. 5 and 6. As shown in the figures, the error w as smaller when the displacement load was 60 mm than when it was 30 mm.

4. Results and discussion

This study applied the metamodel-based optimization technique to optimize the elastomeric bearing in the LMU. In addition, an ideal function was selected to obtain desirable objective values, which were then analyzed and compared with the predicted values. The algorithm was implemented in Excel. The goal was to minimize the error between the objective function (y_t) and approximate function ($\hat{y_i}$) by performing the optimization.

The most important design requirement of the elastomeric bearing is to have the force-displacement curve close to a linear shape. The load applied to the LMU was arbitrarily set to 10 MN, 20 MN, and 30 MN. These values were not only within the actual applied loads but also values in the boundary at the reinforced plate 1, 2, and 3[8, 9].

When the size and number of reinforced plates are increased excessively, it makes the force-displacement curve become nonlinear. Considering this, the design goal was to find the

design variables that made the force-displacement curve closer to linearity. Thus, optimization was performed to minimize the error between ideal function values and predicted function values, as presented in Eq. (1). In particular, this study emphasized the stiffness when displacement was 30 mm and 60 mm, which were regarded as important when performing the optimization. Figs. 7-9 show the comparison results between ideal function and predicted function values at the maximum loads of 10 MN, 20 MN, and 30 MN in the initial design. The results of optimization of the elastomeric bearing according to the maximum load value are presented in Table 4, and RFs with regard to the applied weighted values to obtain the ideal function values are marked in Table 5. As described above, the stiffness at 30 mm and 60 mm of displacement was mainly considered. In particular, a weighted value with regard to 60 mm was increased to the maximum to match the final stiffness. These weighted values were determined through several optimization tries. The errors of the predicted and analysis values with regard to the optimal values are presented in Table 6.

Using the results, a flexible bearing design can be achieved with regard to loads applied in real sites. To show the errors of the predicted and analyzed results according to the maximum loads visually, Figs. 10, 11, and 12 are presented with graphs. The optimal solution provides a combination that makes the force-displacement curve as close to linearity as possible at the given condition.

Table 4 Optimum values according to the max. loads

Applied force	Optimum Values		
	t [mm]	w [mm]	n [ea]
10MN	7.04	200.0	1
20MN	9.0	189.0	2
30MN	3.0	185.5	3

Table 5 Reaction force according to the max. loads

Applied force	δ	30mm	60mm
	WF	30.0	100.0
10MN	RF (kN)	3208.7	10165.7
20MN		5497.2	20259.9
30MN		7833.9	30470.5

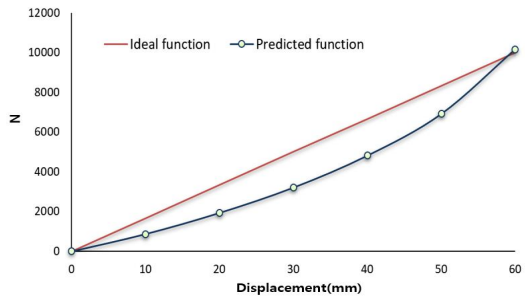

Fig. 7 Comparison of predicted function and ideal function at 10MN

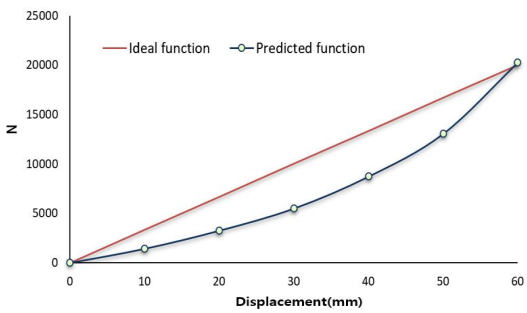

Fig. 8 Comparison of predicted function and ideal function at 10MN

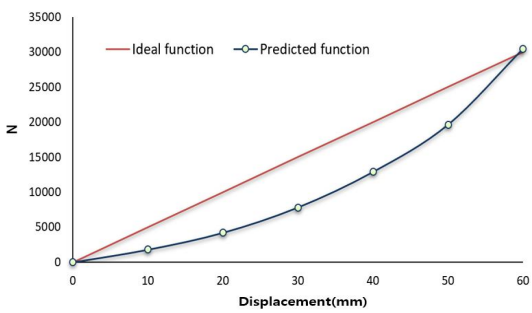

Fig. 9 Comparison of predicted function and ideal function at 10MN

Table 6 Comparison of optimum and analysis result

Maximum Force		RF(kN)	
		30mm	60mm
10MN	Prediction	3208.7	10165.7
	Analysis	3207	10323
Erorr(%)		0.05	1.52
20MN	Prediction	5497.2	20259.9
	Analysis	5119	18855
Erorr(%)		7.39	7.45
30MN	Prediction	7833.9	30470.5
	Analysis	7058	29184
Erorr(%)		10.0	4.4

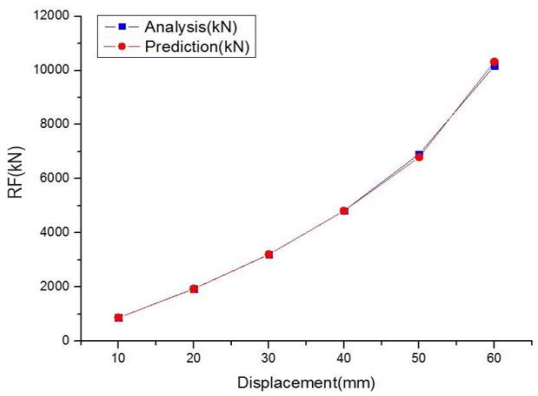

Fig. 10 Load-Displacement curve at 10MN

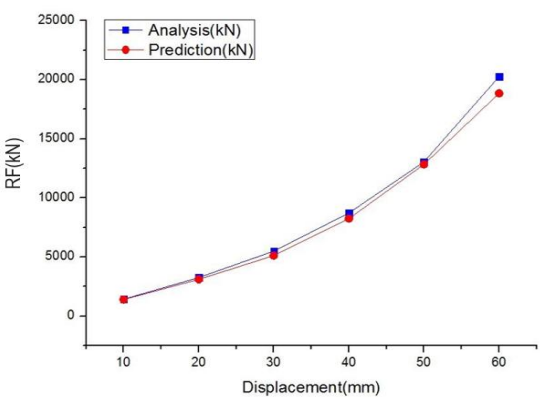

Fig. 11 Load-Displacement curve at 20MN

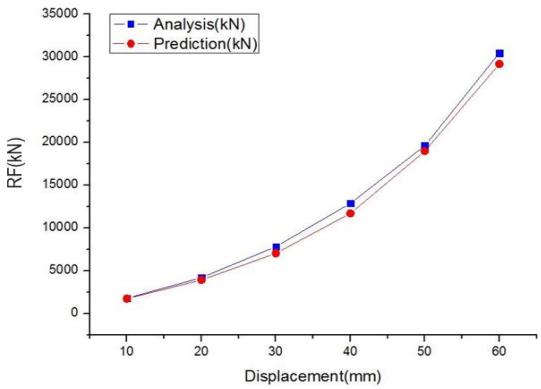

Fig. 12 Load-Displacement curve at 30MN

5. Conclusions

This study optimized an elastomeric bearing in an LMU, which is required to install marine structures and absorb impact at the supporting point of marine structures, and obtained the following conclusions.

1) The stiffness could be predicted with a function of design variables using the Kriging approximate model. To do this, the experimental design and Kriging approximate model were applied.
2) The comparison results of the predicted and analysis values with regard to stiffness showed that a reliable approximate model was developed.
3) The optimal solution was obtained that satisfied the design requirement of the ideal elastomeric bearing (i.e., to make the force-displacement curve as close to linearity as possible within the given design range).
4) When the applied load was 10 MN, t=7.04 (mm), w=200 (mm), and n=1 (ea.); when it was 20 MN, t=9 (mm), w=189 (mm), and n=2 (ea.); and when it was 30 MN, t=3 (mm), w=185.53 (mm), and n=3 (ea.). The design procedure proposed in this study can achieve the flexible design of elastomeric bearings.

Acknowledgment

This research was supported by Basic Science Research Program through the National Research Foundation of Korea(NRF) funded by the Ministry of Education(No. 2017R1D1A3B03029727).

REFERENCES

1. Han, D. S., Jang, S. H., Lee, K. H., “Stiffness Evaluation of Elastomeric Bearings for Leg Mating Unit,” Journal of the Korea Academia-Industrial Cooperation Society, Vol. 18, No. 12, pp. 106-111, 2017.
2. Sin, B. S., Kim, S. U., Kim J. K., Lee, K. H., “Robust Design of an Automobile Ball Joint Considering the Worst-Case Analysis,” Journal of the Korean Society of Manufacturing, Vol. 16, No. 1, pp. 102-111, 2017.
3. Nestor, V. Q., Javier, V. G., Salvador, P., “Surrogate Modeling-Based Optimization of SAGD Processes,” Journal of Petroleum Science and Engineering, Vol. 35, Issues 1 – 2, pp. 83-89, 2002.
4. Song, B. C., Park, Y. C., Kang, S. W., Lee, K. H., “Structural Optimization of an Upper Control Arm, Considering the Strength,” J. of Automobile Engineering, Vol. 223, No. 6, pp. 727-735, 2009.
5. Lee, K. H., “A Robust Structural Design Method Using the Kriging Model to Define the Probability of Design Success,” Journal of Mechanical Engineering Science, Series C, Vol. 224, No. 2, pp. 379-388, 2010.
6. Park, Y. C., Baek, S. K., Seo, B. K., Kim, J. K., Lee, K. H., “Lightweight Design of an Outer Tie Rod for an Electrical Vehicle,” Journal of Applied Mathematics, Vol. 2014, pp. 6, 2014.
7. Byon, S. K., “Optimization of Boss Shape for Damage Reduction of the Press-fitted Shaft End,” Journal of the Korean Society of Manufacturing, Vol. 14, No. 3, pp. 85-91, 2015 (http://doi.org/10.14775/ksmpe.2015.14.3.085).
8. Bae, D. Y., Lee, S. J., Lee, J. Y., “Calculation of Load on Jacket Leg during Float-over Installation of Dual Topsides Using Single Vessel,” Journal of Ocean Engineering and Technology, Vol. 29, No. 2, pp. 135-142, 2015.
9. Seval, P., Fuad, O., “Compression of Hollow-Circular Fiber-Reinforced Rubber Bearings,” Structural Engineering and Mechanics, Vol. 38, No. 3, pp. 361-384, 2011.